PROCEEDINGS OF SCIENCE

SUSY searches with the ATLAS detector

Vasiliki A. Mitsou*
Instituto de Física Corpuscular (IFIC), CSIC – Universitat de València,
Parc Científic de la U.V., C/ Catedrático José Beltrán 2,
E-46980 Paterna (Valencia), Spain
E-mail: vasiliki.mitsou@ific.uv.es

Supersymmetry (SUSY) is one of the most relevant scenarios of new physics searched for by the ATLAS experiment at the CERN Large Hadron Collider (LHC). In this paper the principal search strategies employed by ATLAS are outlined and the most recent results for analyses targeting SUSY discovery are presented. A wide range of signatures are covered motivated by various theoretical scenarios and topologies: strong production, third-generation fermions, electroweak production and R-parity violation among others. Most results are based on $\sim 13-18$ fb^{-1} of data recorded in 2015 – 2016 at $\sqrt{s} = 13$ TeV centre-of-mass energy by the ATLAS experiment at the LHC.

Corfu Summer Institute 2016 "School and Workshops on Elementary Particle Physics and Gravity"
31 August - 23 September, 2016
Corfu, Greece

*Speaker.

PoS(CORFU2016)133

1. Introduction

Supersymmetry (SUSY) [1] is an extension of the Standard Model (SM) which assigns to each SM field a superpartner field with a spin differing by a half unit. SUSY provides elegant solutions to several open issues in the SM, such as the hierarchy problem, the identity of dark matter, and the grand unification.

SUSY searches in collider experiments typically focus on events with high transverse missing energy ($E_{\mathrm{T}}^{\mathrm{miss}}$) which can arise from the (weakly interacting) lightest supersymmetric particle (LSP), in the case of R-parity conserving SUSY, or from neutrinos produced in LSP decays, when R-parity is broken. Hence, the event selection criteria of inclusive channels are based on large $E_{\mathrm{T}}^{\mathrm{miss}}$, no or few leptons ($e$, μ), many jets and/or b-jets, τ-leptons and photons. The exact sets of cuts ("signal regions") are a compromise between the necessity to suppress events coming from known SM processes while maintaining sufficient number of surviving SUSY events. Typical SM backgrounds are top-quark production —including single-top—, W/Z in association with jets, dibosons and QCD multi-jet events. These are estimated using semi- or fully data-driven techniques. Although the various analyses are motivated and optimised for a specific SUSY scenario or topology, the interpretation of the results may be extended to various SUSY models.

A summary of recent results (as of September 2016) on searches for SUSY with and without R-parity conservation is presented. The majority of the reported results are based on up to ~ 18 fb^{-1} of data from pp collisions at a centre-of-mass energy of $\sqrt{s} = 13$ TeV recorded in 2015 – 2016 by ATLAS [2] at the Large Hadron Collider (LHC) [3]. Analyses exploring R-parity conserving SUSY models are currently divided into inclusive searches for: (a) squarks and gluinos, (b) third-generation fermions, and (c) electroweak production ($\tilde{\chi}^0$, $\tilde{\chi}^{\pm}$, $\tilde{\ell}$). Recent results from each category of ATLAS searches are presented in Sections 2, 3 and 4, respectively. Searches designed to look for R-parity violating models are discussed in Section 5. Section 6 summarises the results presented here.

2. Squarks and gluinos

Strong SUSY production is searched in events with large jet multiplicities and large missing transverse momentum, with and without leptons. Various channels fall into this class of searches; here four cases are showcased: the 0-lepton channel; leptonic signatures; the fully hadronic multijet final state; and the photon plus $E_{\mathrm{T}}^{\mathrm{miss}}$ channel.

In the 0-lepton search [4], two selection strategies to search for the supersymmetric partners of quarks and gluons (squarks and gluinos) in final states containing hadronic jets, missing transverse momentum but no electrons or muons are presented. The data used for both approaches were recorded in 2015 and 2016 by the ATLAS experiment in $\sqrt{s} = 13$ TeV proton-proton collisions at the LHC, corresponding to an integrated luminosity of 13.3 fb^{-1}. The first approach summarises the most recent search results of the analysis [5], which is based on the effective mass, m_{eff}. The second is the complementary search using Recursive Jigsaw Reconstruction (RJR) techniques [6] in the construction of a discriminating variable set *(RJR-based search)*. By using a dedicated set of selection criteria, the RJR-search improves the sensitivity to supersymmetric models with small mass splittings between the sparticles (models with compressed spectra). Both searches adopt the same analysis strategy as the previous ATLAS search designed for the analysis of the 7 TeV, 8 TeV and 13 TeV data collected during Run 1 and Run 2 of the LHC.

Due to the high mass scale expected for the SUSY models considered in this study, the effective mass, m_{eff}, is a powerful discriminant between the signal and SM backgrounds. When selecting events with at least N_j jets, $m_{\mathrm{eff}}(N_j)$ is defined to be the scalar sum of the transverse momenta of the leading N_j jets and $E_{\mathrm{T}}^{\mathrm{miss}}$. Requirements placed on m_{eff} and $E_{\mathrm{T}}^{\mathrm{miss}}$ form the basis of the m_{eff}-based search by strongly suppressing the multi-jet background where jet energy mismeasurement generates missing transverse momentum. The final signal selection uses requirements on both $m_{\mathrm{eff}}(\mathrm{incl.})$, which sums over all jets with $p_{\mathrm{T}} > 50$ GeV and $E_{\mathrm{T}}^{\mathrm{miss}}$, which is required to be larger than 250 GeV. An example of a $m_{\mathrm{eff}}(\mathrm{incl.})$ distribution for a specific signal region is plotted in Fig. 1.

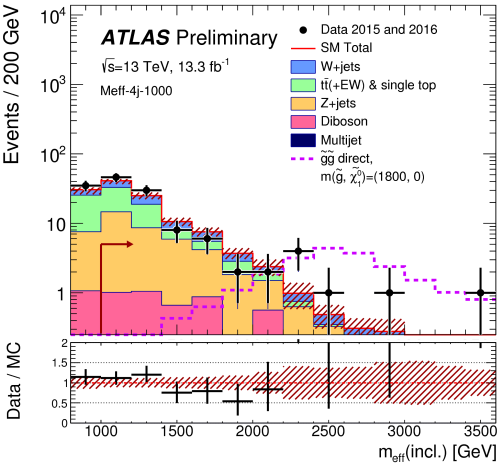

Figure 1: Observed $m_{\mathrm{eff}}(\mathrm{incl.})$ distributions for the Meff-4j-1000 signal region of the 0-lepton analysis. The histograms denote the MC background expectations prior to the fits described in the text, normalised to cross-section times integrated luminosity. The hatched (red) error bands denote the combined experimental, MC statistical and theoretical modelling uncertainties. The arrows indicate the values at which the requirements on $m_{\mathrm{eff}}(\mathrm{incl.})$ are applied. Expected distributions for benchmark model points, normalised to NLO+NLL cross-section times integrated luminosity, are also shown for comparison (masses in GeV). From [4].

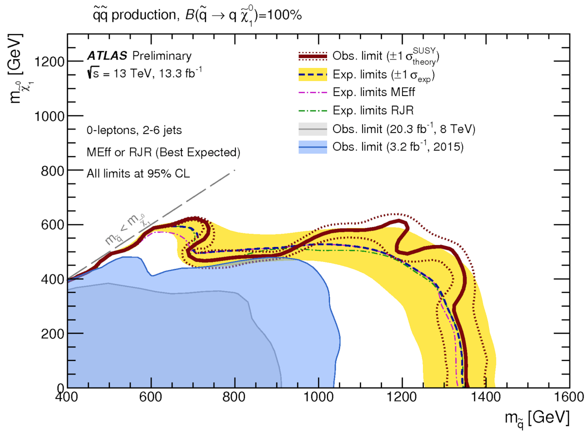

Figure 2: Exclusion limits for direct production of light-flavour squark pairs with decoupled gluinos acquired with the 0-lepton search. Gluinos are required to decay to two quarks and a neutralino LSP. The blue dashed lines show the expected limits at 95% CL, with the light (yellow) bands indicating the 1σ excursions due to experimental and background-only theoretical uncertainties. Observed limits are indicated by medium dark (maroon) curves where the solid contour represents the nominal limit, and the dotted lines are obtained by varying the signal cross-section by the renormalisation and factorisation scale and PDF uncertainties. Results are compared with the observed limits obtained by the previous ATLAS searches with no leptons, jets and missing transverse momentum. From [4].

The results are interpreted in the context of various simplified models where squarks and gluinos are pair-produced and the neutralino is the lightest supersymmetric particle. An exclusion limit at the 95% confidence level (CL) on the mass of the gluino is set at 1.86 TeV for a simplified model incorporating only a gluino octet and the lightest neutralino, assuming the lightest neutralino is massless. For a simplified model involving the strong production of mass-degenerate first-and second-generation squarks, squark masses below 1.35 TeV are excluded for a massless lightest neutralino, as shown in Fig. 2. Exclusion limits are obtained by using the signal region with the best expected sensitivity at each point. Expected limits from the $M_{\mathrm{eff}-}$ and RJR-based searches separately are also shown for comparison. These limits substantially extend the region of supersymmetric parameter space excluded by previous measurements with the ATLAS detector.

The experimental signature characterising the 1-lepton search [7] consists of a lepton (electron or muon) from the decay of one of the W bosons, several jets, and missing transverse momentum from the undetectable neutralinos and neutrino(s). In a similar fashion, the 2-lepton analysis with two opposite-sign leptons [8] is motivated by the decay of a Z boson. The number of detectable leptons and jets and their kinematics depend on the mass and the identity (gluinos or squarks) of the pair-produced sparticles as well as on the masses of the lightest chargino and the neutralino. Ten sets of signal selection criteria, or signal regions (SRs), are defined in order to provide sensitivity to a broad range of mass spectra in both models. In each SR, the event yield is compared against the expectation from the SM processes, which is estimated using a combination of simulation and observed data in control regions (CRs). The search uses the ATLAS data collected in proton-proton collisions at the LHC in 2015 and 2016 at a centre-of-mass energy of 13 TeV, corresponding to an integrated luminosity of 14.8 fb^{-1}.

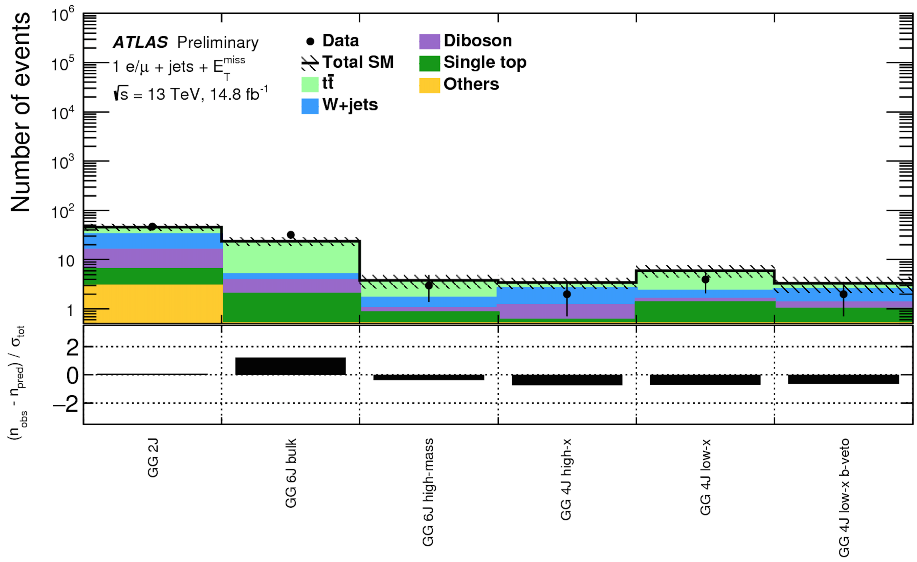

Figure 3: 1-lepton analysis: Expected background yields as obtained in the background-only fits in gluino signal regions together with observed data are given in the top parts of the plot. Uncertainties in the fitted background estimates include both statistical (in the simulated event yields) and systematic uncertainties. The bottom parts of the plots show the differences between observed (n_{obs}) and predicted (n_{pred}) event yields, divided by the total uncertainty in the prediction (σ_{tot}). From [7].

The observed data agree with the Standard Model background prediction in the signal regions, as shown in Fig. 3. For all signal regions, limits on the visible cross-section are derived in models of new physics within the kinematic requirements of this search. In addition, exclusion limits are placed on models with squark- or gluino-pair production and subsequent decays via an intermediate chargino to the lightest neutralino. Limits of previous searches conducted in LHC Run 1 are significantly extended. Gluino (squark) masses up to 1.8 TeV (1.1 TeV) are excluded for low neutralino masses ($\lesssim$ 400 GeV or $\lesssim$ 300 GeV) and chargino masses of $\sim$ 930 GeV (470 GeV or 650 GeV).

Reference [9] documents a search for new phenomena with large jet multiplicities (from ≥ 8 to ≥ 10) and missing transverse momentum, where the jets are consistent with coming from the decays of heavy objects, so they can be clustered into a smaller number of high-mass, M_J^Σ, jets. The search uses 18.2 fb^{-1} of $\sqrt{s} = 13$ TeV pp collision data collected by ATLAS at the LHC. The increase in the LHC centre-of-mass energy with respect to Run 1 provides increased sensitivity to higher-mass sparticles. The sensitivity to new physics is enhanced by considering the scalar sum of masses of radius $R = 1.0$ jets in the event, reconstructed using the anti-k_t clustering algorithm. The Standard Model predictions are found to be consistent with the data (cf. Fig. 4). The results are interpreted in the context of a simplified supersymmetry model, and a slice of the pMSSM (cf. Fig. 5), each of which predict cascade decays of supersymmetric particles and hence large jet multiplicities. The data exclude gluino masses up to 1600 GeV at the 95% CL, extending previous bounds. Model-independent limits are presented which allow reinterpretation of the results to cases of other models which also predict decays into multijet final states in association with invisible particles.

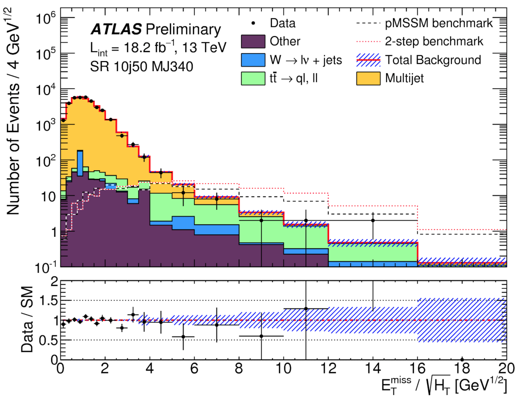

Figure 4: Multijet selection: Distributions of the selection variable $E_{\mathrm{T}}^{\mathrm{miss}}/\sqrt{H_{\mathrm{T}}}$ for events with at least 10 jets and $M_J^\Sigma > 340$ GeV. The dashed lines indicate the prediction for several different simplified model scenarios for different gluino and χ_1^0 masses. The sub-plots show the ratio of the data to the SM prediction. The blue hatched band shows the statistical uncertainty arising from a finite number of MC events and limited data in the templates and $E_{\mathrm{T}}^{\mathrm{miss}}/\sqrt{H_{\mathrm{T}}} < 1.5$ normalisation regions. The dashed lines labelled pMSSM and 2-Step refer to benchmark signal points — a pMSSM slice model with $(m(\tilde{g}), m(\tilde{\chi}_1^\pm)) = (1400, 200)$ GeV and a cascade decay model with $(m(\tilde{g}), m(\tilde{\chi}_1^0)) = (1400, 200)$ GeV. From [9].

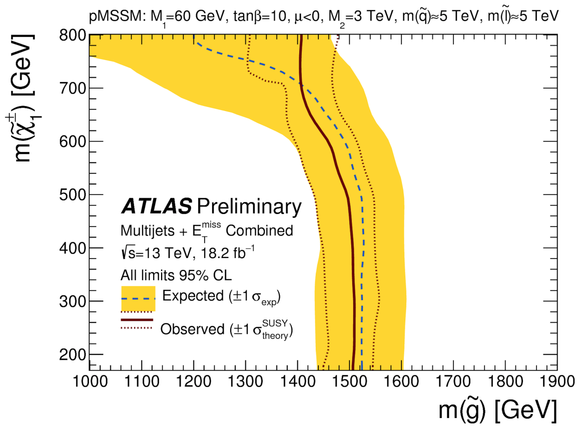

Figure 5: Multijet selection: The 95% CL exclusion curves for the pMSSM model. The solid red and dashed blue curves show the 95% CL observed and expected limits, respectively, including all uncertainties except the theoretical signal cross-section uncertainty (PDF and scale). The dotted red lines bracketing the observed limit represent the result produced when moving the signal cross-section by $\pm 1\sigma$ (as defined by the PDF and scale uncertainties). The shaded yellow band around the expected limit shows the $\pm 1\sigma$ variation of the expected limit. The shaded grey area shows the observed exclusion from a previous ATLAS analysis. Excluded regions are below and to the left of the relevant lines. From [9].

A search for the experimental signature of isolated high-p_T photons, jets and high missing transverse momentum has been performed using 13.3 fb^{-1} of pp collision data at $\sqrt{s} = 13$ TeV produced by the LHC and collected by the ATLAS detector in 2015 and 2016 [10]. Two different signal regions, $\mathrm{SR_L}$ and $\mathrm{SR_H}$, were designed for the present search. $\mathrm{SR_L}$ is optimised for high mass gluino and a low/intermediate mass neutralino and $\mathrm{SR_H}$ targets those scenarios where the gluino and neutralino masses are close to each other. Three events are observed in $\mathrm{SR_L}$ and one event in $\mathrm{SR_H}$ (cf. Fig. 6), where the estimated SM background are 0.78 and 1.49, respectively. Within the statistical and systematic uncertainties, the observed results are consistent with the Standard Model. In a GGM scenario with a NLSP neutralino that is a mixture of higgsino and bino, a lower limit is set on the mass of a degenerate octet of gluino states of 1800 GeV for a large range of neutralino masses, increasing to 2000 GeV in the case of a high mass neutralino, as shown in Fig. 7.

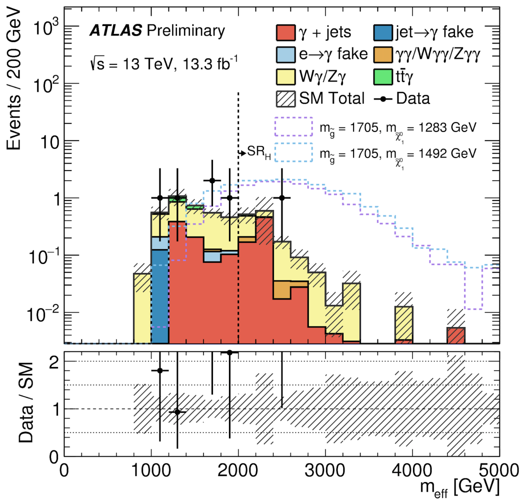

Figure 6: Photon plus jets analysis: Observed (points with error bars) and expected background (solid histograms) distributions for m_{eff} in the signal region $\mathrm{SR_H}$ after the background-only fit. The predicted signal distributions for two selected values of the the gluino and neutralino masses are also shown for comparison. From [10].

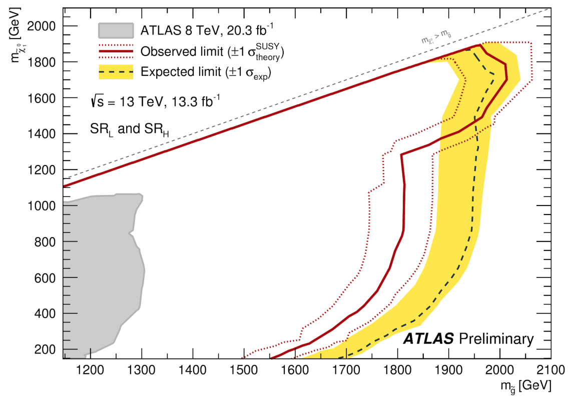

Figure 7: Photon plus jets analysis: Observed and expected exclusion limit at 95% CL for $\mathrm{SR_L}$ and $\mathrm{SR_H}$ analyses using the signal region with the best expected sensitivity at each point, for 2015+2016 data corresponding to an integrated luminosity of 13.3 fb^{-1}. From [10].

3. Third-generation squarks

The mixing of left- and right-handed gauge states which provides the mass eigenstates of the scalar quarks and leptons can lead to relatively light 3$^{\mathrm{rd}}$ generation particles. Stop ($\tilde{t}_1$) and sbottom ($\tilde{b}_1$) with a sub-TeV mass are favoured by the naturalness argument, while the stau ($\tilde{\tau}_1$) is the lightest slepton in many models. Therefore these could be abundantly produced either directly or through gluino production and decay. Such events are characterised by several energetic jets (some of them b-jets), possibly accompanied by light leptons, as well as high E_T^{miss}.

The results of a search for the stop, the supersymmetric partner of the top quark, in final states with one isolated electron or muon, jets, and missing transverse momentum are reported in Ref. [11]. The search uses the LHC pp collision data collected in 2015 and 2016 at a centre-of-mass energy of $\sqrt{s} = 13$ TeV recorded by the ATLAS detector corresponding to an integrated luminosity of 13.2 fb^{-1}. The stop decay scenarios considered are those to a top quark and the lightest neutralino as well as to a bottom quark and the lightest chargino, followed by the chargino decays to the lightest neutralino and a W boson. A range of scenarios with different mass splittings between the stop, the lightest chargino and the lightest neutralino are considered. The analysis also targets the production of dark matter in association with a pair of top quarks using the same final state. The largest deviation from the Standard Model prediction is found in one of the seven signal selections, the DM_low, shown in Fig. 8, where 35 events are observed with 17 ± 2 background events expected, corresponding to a local significance of 3.3 standard deviations. A stop with a mass of 830 GeV decaying directly to a top quark and a massless neutralino is excluded at 95% confidence level. Stringent exclusion limits are also derived for all other considered stop decay scenarios, and upper limits are set on the visible cross-section for processes beyond the Standard Model.

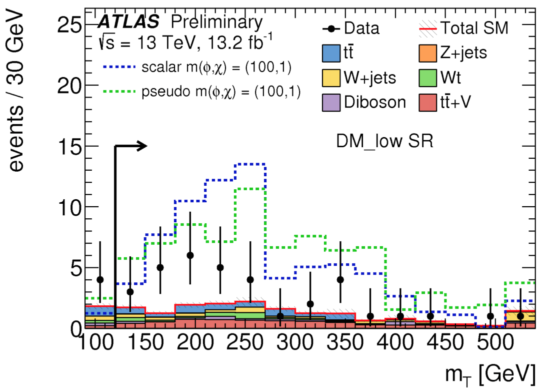

Figure 8: The m_T distribution in DM_low for the stop 1-lepton search. The full event selection in the corresponding signal region is applied, except for the requirement (indicated by an arrow) imposed on m_T. The uncertainty band includes statistical uncertainties. The last bin contains the overflow. Benchmark signal models where a common coupling $g = g_q = g_\chi = 3.5$ is assumed are overlaid for comparison. From [11].

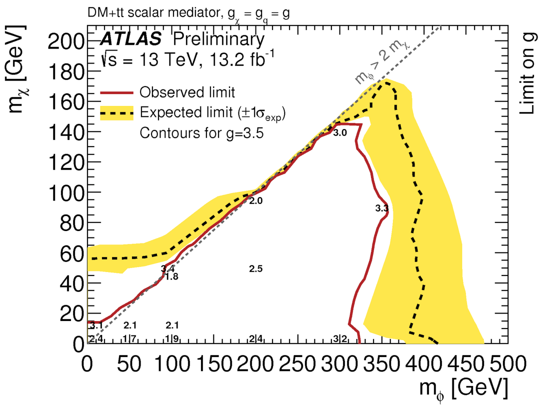

Figure 9: Stop 1-lepton search: The observed upper limit on the couplings in the plane of m_ϕ versus m_χ dark matter associated production with top quarks for a scalar mediator. The observed and expected lines correspond to the limit for the coupling $g = 3.5$. Numbers on the plot show the value of the coupling. The coupling being shown and the coupling above are excluded at 95% CL for the corresponding points on the signal grid. From [11].

For the dark matter search, limits are obtained for the common coupling value of $g = 3.5$ in a plane of dark matter particle mass and a scalar or pseudo-scalar mediator mass. The maximal coupling of $g = 3.5$ is excluded at 95% confidence level for a scalar (pseudo-scalar) mediator mass up to 320 (350) GeV assuming a 1 GeV dark matter particle mass, as shown in Fig. 9.

The exclusion limits imposed by several searches for the direct production of a top super-partner decaying to a neutralino LSP are summarised in Fig. 10. The decay mode $\tilde{t}_1 \to b + \tilde{\chi}_1^\pm$ with $\tilde{\chi}_1^\pm \to W^{(*)\pm} + \tilde{\chi}_1^0$ is assumed with 100% branching ratio. Various hypotheses on the $\tilde{t}_1$, $\tilde{\chi}_1^\pm$ and $\tilde{\chi}_1^0$ mass hierarchy are used: fixed $\tilde{\chi}_1^\pm$ mass (106 GeV, 150 GeV), $m(\tilde{\chi}_1^\pm) \sim 2 \times m(\tilde{\chi}_1^0)$, fixed $\Delta M = m(\tilde{t}_1) - m(\tilde{\chi}_1^\pm)$ at 10 GeV, and fixed $\Delta M = m(\tilde{\chi}_1^\pm) - (\tilde{\chi}_1^0)$ at 5 GeV. Note that these plots overlay contours belonging to different stop decay channels, different sparticle mass hierarchies, and simplified decay scenarios, hence care must be taken when interpreting them.

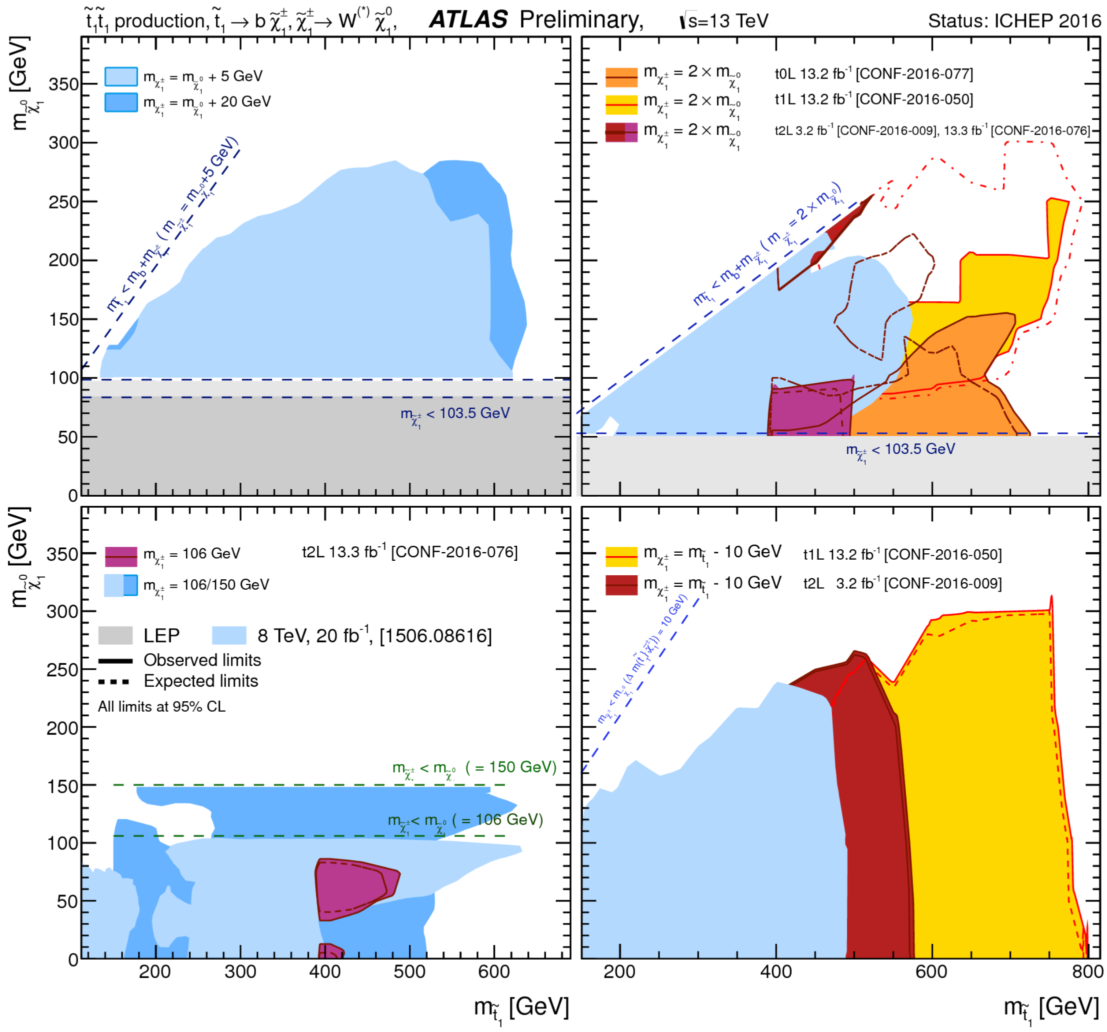

Figure 10: Summary of the dedicated ATLAS searches for top squark (stop) pair production based on 13 fb^{-1} of pp collision data taken at $\sqrt{s} = 13$ TeV. Exclusion limits at 95% CL are shown in the $(\tilde{t}_1, \tilde{\chi}_1^0)$ mass plane. The dashed and solid lines show the expected and observed limits, respectively, including all uncertainties except the theoretical signal cross section uncertainty (PDF and scale). From [12].

4. Electroweak gaugino production

Electroweak SUSY production is motivated by naturalness and it is complementary to search focusing on strongly produced sparticles. Natural models of SUSY favour light chargino and neutralino masses, in a range well accessible at the LHC. In the event that the strong production is sufficiently heavy, electroweak SUSY production may be the dominant SUSY production mechanism at the LHC. Two recent analyses with 13-TeV data are highlighted here together with the interpretation of Run-1 electroweak (EW) searches in terms of dark matter models.

Reference [13] reports on the searches for direct production of opposite-sign pair of the lightest charginos ($\tilde{\chi}_1^+\tilde{\chi}_1^-$) and the pair production of the lightest chargino with the next-to-the-lightest neutralino ($\tilde{\chi}_1^\pm\tilde{\chi}_2^0$) using 13.3 fb^{-1} of integrated luminosity from LHC pp collisions at $\sqrt{s} = 13$ TeV collected by the ATLAS detector. These studies have been performed in final states including two and three leptons (electrons or muons) and large missing transverse momentum. The results have been found to be in agreement with the Standard Model expectations. Exclusion limits at 95% CL are derived on the masses of the $\tilde{\chi}_1^\pm/\tilde{\chi}_2^0$ (assumed to be mass degenerate) and the lightest neutralino ($\tilde{\chi}_2^0$) assuming 100% branching ratio of the $\tilde{\chi}_1^\pm$ and $\tilde{\chi}_2^0$ to sleptons ($\tilde{\ell}$). These results extend the region of supersymmetric parameter space excluded by the Run 1 LHC searches. For the case of $\tilde{\chi}_1^+\tilde{\chi}_1^-$ scenario the observed limit on the $m_{\tilde{\chi}_1^\pm}$ is at 620 GeV (cf. Fig. 11) while for the case of $\tilde{\chi}_1^\pm\tilde{\chi}_2^0$ the observed limit on $m_{\tilde{\chi}_1^\pm/\tilde{\chi}_2^0}$ has been extended to 1 TeV for massless $\tilde{\chi}_1^0$.

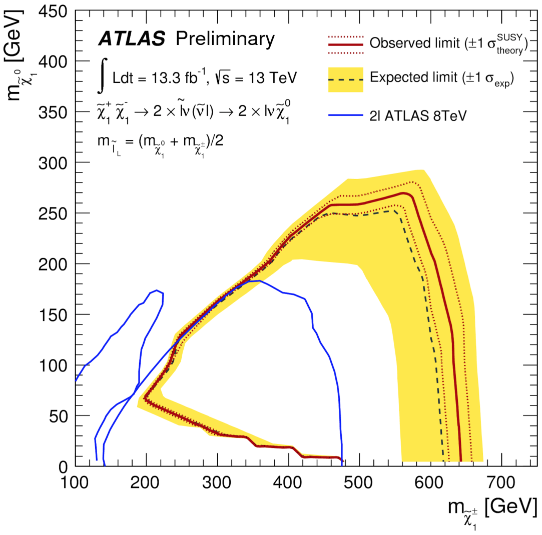

Figure 11: 95% CL exclusion limits on the common $\tilde{\chi}_1^\pm$ and $\tilde{\chi}_1^0$ masses for simplified models and direct $\tilde{\chi}_1^+\tilde{\chi}_1^-$ pair production using the two-lepton signal regions. The contours of the band around the expected limit are the $\pm 1\sigma$ results, including all uncertainties except theoretical uncertainties on the signal cross-section. The dotted lines around the observed limit illustrate the change in the observed limit as the nominal signal cross-section is scaled up and down by the theoretical uncertainty. Results are compared with the observed limits obtained by previous ATLAS searches. From [13].

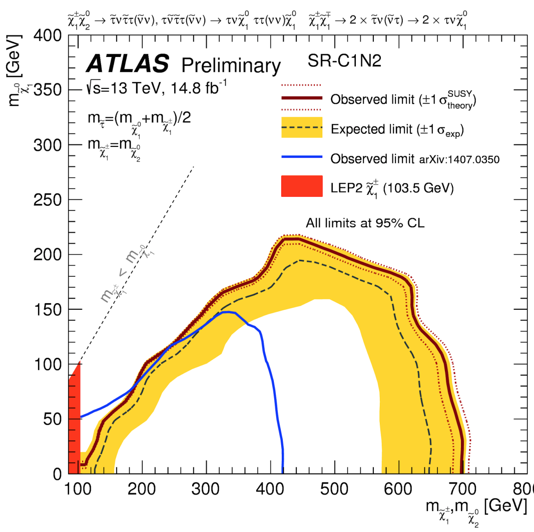

Figure 12: EW-production two-tau analysis: Observed and expected exclusion limits in the context of SUSY scenarios with simplified mass spectra with associated production of $\tilde{\chi}_1^+\tilde{\chi}_1^-$ and $\tilde{\chi}_1^\pm\tilde{\chi}_2^0$. See Fig. 11 caption for details on exclusion curves and uncertainty bands. All limits are computed at 95% CL. The LEP limit on the chargino mass is also shown. The observed limits obtained from ATLAS during LHC Run 1 are also shown as blue contours. From [14].

Searches for the electroweak production of charginos and neutralinos in final states with at least two hadronically decaying tau leptons have been performed [14]. The analysis uses a dataset of proton-proton collisions corresponding to an integrated luminosity of 14.8 fb^{-1}, recorded with the ATLAS detector at the LHC at a centre-of-mass energy of $\sqrt{s} = 13$ TeV. No significant deviation from the Standard Model expectation was observed. Limits are derived in scenarios of $\tilde{\chi}_1^+\tilde{\chi}_1^-$ pair production and $\tilde{\chi}_1^\pm\tilde{\chi}_2^0$ and $\tilde{\chi}_1^+\tilde{\chi}_1^-$ associated production. Common $\tilde{\chi}_1^\pm - \tilde{\chi}_2^0$ masses up to 580 and 700 GeV respectively are excluded at 95% CL assuming a massless $\tilde{\chi}_1^0$ (cf. Fig. 12).

Furthermore electroweak production of sparticles may probe dark matter models [15]. Reference [16] summarises the combined sensitivity and constraints from 22 separate ATLAS analyses of the Run 1 LHC dataset [17]. The interpretation of those results is done here within the wider framework of the pMSSM, where the over a hundred parameters of the MSSM are reduced to 19 applying a series of assumptions motivated by either experimental constraints or general features of possible SUSY breaking mechanisms. The model is assumed to conserve R-parity and the LSP is assumed to be the lightest neutralino. A total of 310,327 model points are selected, each of which satisfies constraints from previous collider searches, precision measurements, cold dark matter energy density measurements and direct dark matter searches.

The impact of the ATLAS Run 1 searches on this model space is presented in Fig. 13, showing their overall effect in constraining such supersymmetric models. The plot shows the fraction of model points excluded for each sparticle as a function of $\tan\beta$ parameter.

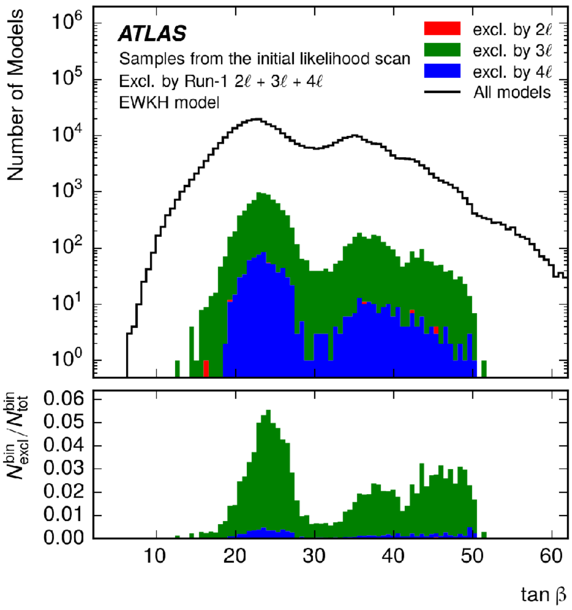

Figure 13: The number of models sampled by the initial likelihood scan, and the stacked bin-by-bin number of models excluded by the Run 1 ATLAS SUSY searches as a function of $\tan\beta$. The lower part of the figure shows the fraction of excluded models by the Run 1 ATLAS SUSY searches. The red bins indicates the fraction that is excluded by a 2ℓ SR, the green by a 3ℓ SR, and blue by a 4ℓ SR. The models considered are all within the 1D 95% confidence interval found using the initial likelihood scan. The plots are truncated in $|M_1|$ and $|\mu|$ to highlight the region of ATLAS electroweak SUSY sensitivity. From [16].

5. *R*-parity violating SUSY

R parity is defined as $R = (-1)^{3(B-L)+2S}$, where B (L) is the baryon (lepton) number and S the spin, respectively, granting $R = +1$ ($R = -1$) to all SM particles (SUSY partners). It is worth emphasising that the conservation of R parity is merely an *ad-hoc* assumption with the only strict limitation coming from the proton lifetime: non-conservation of both B and L leads to a rapid proton decay. R-parity conservation has serious consequences in SUSY phenomenology in colliders: the SUSY particles are produced in pairs and, most importantly, the lightest supersymmetric particle (LSP) is absolutely stable and weakly interacting, thus providing the characteristic high transverse missing momentum ($E_{\mathrm{T}}^{\mathrm{miss}}$) in SUSY events at colliders. It is stressed that in view of the null results in *conventional* SUSY searches, it becomes mandatory to fully explore *non-standard* SUSY scenarios also involving R-parity violation (RPV) [18] and/or quasi-stable particles.

Here we highlight some recent analyses targeting RPV scenarios where R parity is broken by trilinear terms $\lambda LL\bar{E}$ or $\lambda'' \bar{U}\bar{D}\bar{D}$. Alternatively, RPV can be induced by *bilinear* terms, εLH_u, which also explain neutrino masses and mixing, rendering it a quite attractive theoretical scenario [19].

In Ref. [20] a benchmark model is considered where wino-like charginos are pair-produced, and the LSP is a bino-like neutralino. The $\tilde{\chi}_1^{\pm}$ decays to the LSP while emitting a W boson, as shown in Fig. 14. The subsequent $\tilde{\chi}_1^0$ decay is mediated by a $\lambda_{ijk}L_iL_j\bar{E}_k$ term in the supersupotential, allowing each LSP to undergo a lepton-number-violating RPV decay to two charged leptons and a neutrino with the allowed lepton flavours depending on the indices of the associated λ_{ijk} couplings. Thus, every signal event contains a minimum of four charged leptons, and potentially up to six if both W bosons decay leptonically. The search is therefore based on a final state with four or more leptons (electrons or muons), no Z boson candidates, and large effective mass. The analysis is based on 13.3 fb^{-1} of proton-proton collision data delivered by the LHC at $\sqrt{s} = 13$ TeV in 2015 and 2016. No significant excess of events is found in data. The null result is interpreted in a simplified model of chargino pair production with indirect RPV decays, where chargino masses up to 1.14 TeV are excluded for large LSP masses, as shown in Fig. 15.

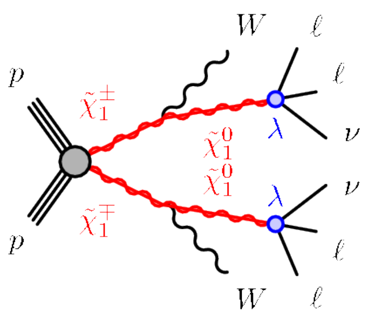

Figure 14: Diagram of the benchmark SUSY model of chargino production with indirect RPV decays. From [20].

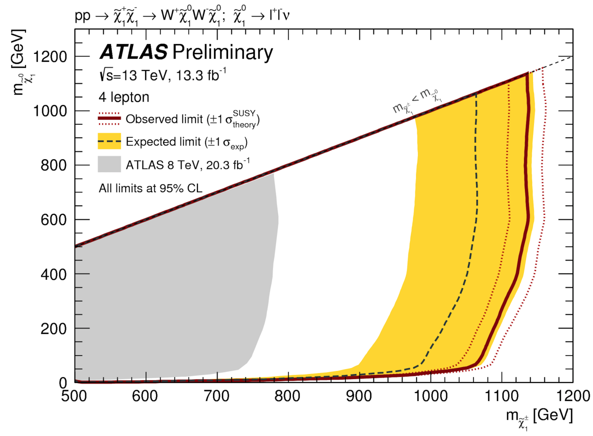

Figure 15: 4-lepton RPV search: The 95% CL exclusion limits on chargino production with indirect RPV decays via λ_{12k}, where $k = 1,2$. The limits are set using the signal region with the best expected exclusion. The 8 TeV limit from a previous analysis is also shown. From [20].

A search for supersymmetric gluino pair productions with subsequent R-parity-violating decays to quarks is presented in Ref. [21]. This search uses 14.8 fb^{-1} of data collected by the ATLAS detector in proton-proton collisions with a centre-of-mass energy of 13 TeV at the LHC. The analysis is performed using both a requirement on the number of jets and the number of jets tagged as containing a b-hadron as well as a topological observable formed from the scalar sum of large-radius jet masses in the event, M_J^{Σ} (cf. Fig. 16). No significant deviation is observed from the expected Standard Model backgrounds. For a model where the gluino decays through an intermediate neutralino which, in turn, decays to three quarks, gluino masses ($m_{\tilde{g}}$) below 1000–1550 GeV are excluded depending on the neutralino mass. Gluinos decaying directly to three quarks are excluded for $m_{\tilde{g}} < 1080$ GeV, as depicted in Fig. 17.

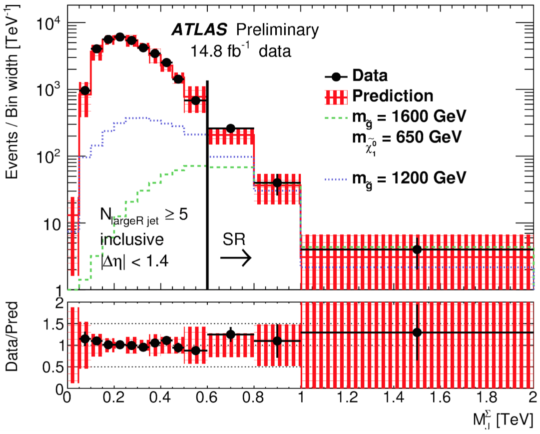

Figure 16: Predicted (solid line) and observed (dots) M_J^Σ distribution for signal region 5jSR of the multijets analysis for RPV SUSY. The shaded area surrounding the predicted M_J^Σ distribution represents the systematic uncertainty of background estimation. The expected contribution from two RPV signal samples are also shown. From [21].

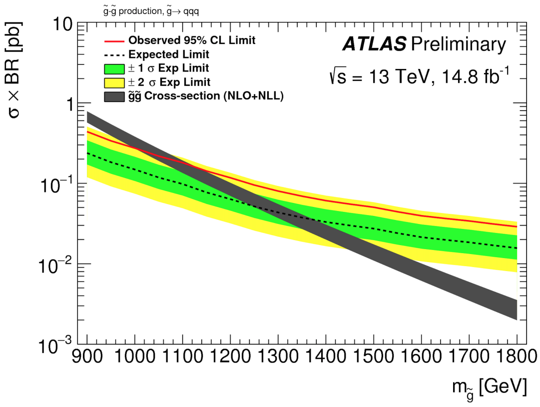

Figure 17: Expected and observed cross-section limits for the gluino direct decay model gluino models applying the results of the multijets analysis for RPV SUSY. From [21].

A search for beyond the Standard Model physics in events with an isolated lepton (electron or muon), high jet multiplicity and no, or many, b-tagged jets is documented in Ref. [22]. Unlike previous searches, no requirement on $E_{\mathrm{T}}^{\mathrm{miss}}$ is applied. A novel data-driven background estimation technique is used to estimate the dominant background from $t\bar{t}$+jets and W/Z+jets production. The analysis is performed with proton-proton collision data at $\sqrt{s} = 13$ TeV collected between August 2015 and July 2016 with the ATLAS detector at the LHC corresponding to an integrated luminosity of 14.8 fb^{-1}. With no significant excess over the Standard Model expectation observed, results are interpreted in the framework of simplified models featuring gluino pair production in R-parity violating supersymmetry scenarios. In a benchmark model with $\tilde{g} \to t\bar{t}\tilde{\chi}_1^0 \to t\bar{t}uds$, gluino masses up to 1.75 TeV are excluded at 95% CL, as demonstrated in Fig. 18. Moreover in a model with $\tilde{g} \to \bar{t}\tilde{t}$ with $\tilde{t} \to bs$, gluino masses up to 1.4 TeV are excluded. In general model-independent limits are set on the contribution of new phenomena to the signal region yields of up to 8 fb at 95% CL.

R-parity violating scenarios may give rise to resonance production, which is not possible in R-parity conserving SUSY due to the invisible LSPs. A search has been performed for the pair production of resonances decaying into two jets, using 15.4 fb^{-1} of data collected by ATLAS at 13 TeV during 2015 and 2016. Four jets are reconstructed and paired into two candidate resonances according to their angular separation. Further selections based on the angular distributions and difference in mass between the two resonances are applied to enhance the fraction of signal. The average mass of the two resonances is used as final discriminant to define signal regions. Both the shape and normalisation of the background are derived from data. No significant excess is observed above the background prediction. The results are interpreted in a SUSY model with pair production of stop quarks decaying into two jets through the λ'' R-parity violating coupling, where

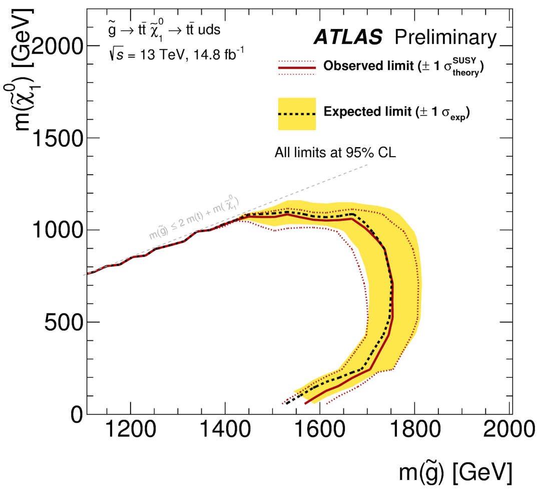

Figure 18: 1-lepton plus multijets RPV analysis: Observed and expected exclusion limits on the gluino and $\tilde{\chi}_1^0$ masses in the context of the RPV SUSY scenarios probed, with simplified mass spectra featuring gluino pair production with exclusive decay modes. The contours of the band around the expected limit are the $\pm 1\sigma$ results, including all uncertainties except theoretical uncertainties on the signal cross section. The dotted lines around the observed limit illustrate the change in the observed limit as the nominal signal cross-section is scaled up and down by the theoretical uncertainty. All limits are computed at 95% CL. The diagonal lines indicate the kinematic limit for the decays in each specified scenario. From [22].

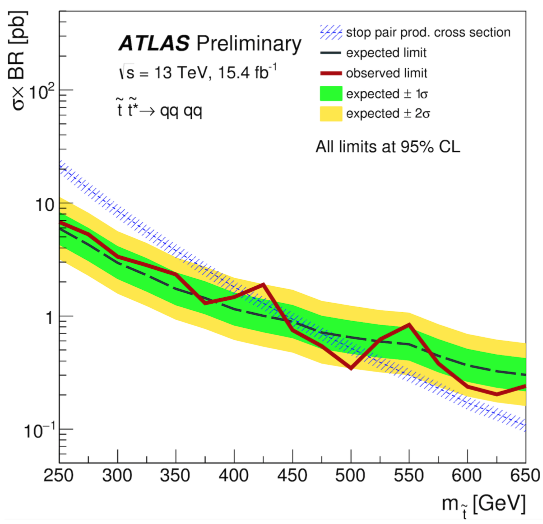

Figure 19: Resonant RPV production search: Expected and observed 95% CL upper limit on the $\sigma \times BR$ for the signal regions, compared to the theoretical cross-section for top squark pair production with decays to a pair of jets. The dashed black and solid red lines show the 95% CL expected and observed limits, respectively. The solid green (yellow) band around the expected limit show the 1 (2) σ uncertainties around this limit. The dashed blue line indicates the nominal top squark production cross-section with the shaded bands representing the one sigma variations due to theoretical uncertainties given by renormalisation and factorisation scale and PDF uncertainties. From [23].

masses of the top squark from 250 to 405 GeV and from 445 to 510 GeV are excluded at 95% CL (cf. Fig. 19). Furthermore in a model of Coloron pair production masses between 250 and 1500 GeV are excluded at 95% CL.

6. Summary

Supersymmetry signals have been sought after by the ATLAS experiment, motivated by various theoretical approaches, models and topologies: strong production, 3$^{\text{rd}}$ generation fermions, electroweak production, mass degeneracies, R-parity violation, among others. They lead to a wide spectrum of signatures: $E_{\mathrm{T}}^{\mathrm{miss}}$ + jets + leptons / photons / b-jets / τ-leptons, displaced vertices, not possible to cover all of them here. No deviation from known SM processes has been observed so far with the data collected during 2015 and 2016 at $\sqrt{s} = 13$ TeV. As both techniques and strategy keep evolving, ATLAS will keep looking for supersymmetry with the new data that become available at the LHC.

Acknowledgments

The author is grateful to the CORFU2016 School organisers for the kind invitation to present this talk. She acknowledges support by the Spanish Ministry of Economy and Competitiveness (MINECO) under the project FPA2015-65652-C4-1-R, by the Generalitat Valenciana through the project PROMETEO II/2013-017, by the Spanish National Research Council (CSIC) under the CT Incorporation Program 201650I002 and by the Severo Ochoa Excellence Centre Project SEV 2014-0398.

References

[1] S. P. Martin, Adv. Ser. Direct. High Energy Phys. **21** (2010) 1 [Adv. Ser. Direct. High Energy Phys. **18** (1998) 1] [hep-ph/9709356].

[2] G. Aad *et al.* [ATLAS Collaboration], JINST **3** (2008) S08003.

[3] L. Evans and P. Bryant, JINST **3** (2008) S08001.

[4] ATLAS Collaboration, ATLAS-CONF-2016-078 (2016).

[5] M. Aaboud *et al.* [ATLAS Collaboration], Eur. Phys. J. C **76** (2016) no.7, 392 [arXiv:1605.03814 [hep-ex]].

[6] P. Jackson, C. Rogan and M. Santoni, Phys. Rev. D **95** (2017) no.3, 035031 [arXiv:1607.08307 [hep-ph]].

[7] ATLAS Collaboration, ATLAS-CONF-2016-054 (2016).

[8] ATLAS Collaboration, ATLAS-CONF-2016-098 (2016); M. Aaboud *et al.* [ATLAS Collaboration], Eur. Phys. J. C **77** (2017) no.3, 144 [arXiv:1611.05791 [hep-ex]].

[9] ATLAS Collaboration, ATLAS-CONF-2016-095 (2016); see also: G. Aad *et al.* [ATLAS Collaboration], Phys. Lett. B **757**, 334 (2016) [arXiv:1602.06194 [hep-ex]].

[10] ATLAS Collaboration, ATLAS-CONF-2016-066 (2016).

[11] ATLAS Collaboration, ATLAS-CONF-2016-050 (2016); see also: M. Aaboud *et al.* [ATLAS Collaboration], Phys. Rev. D **94** (2016) no.5, 052009 [arXiv:1606.03903 [hep-ex]].

[12] ATLAS Supersymmetry public results, https://twiki.cern.ch/twiki/bin/view/AtlasPublic/SupersymmetryPublicResults#summary_plots

[13] ATLAS Collaboration, ATLAS-CONF-2016-096 (2016).

[14] ATLAS Collaboration, ATLAS-CONF-2016-093 (2016).

[15] For a review on dark-matter searches in colliders, see e.g.: V. A. Mitsou, Int. J. Mod. Phys. A **28** (2013) 1330052 [arXiv:1310.1072 [hep-ex]].

[16] M. Aaboud *et al.* [ATLAS Collaboration], JHEP **1609** (2016) 175 [arXiv:1608.00872 [hep-ex]].

[17] G. Aad *et al.* [ATLAS Collaboration], Phys. Rev. D **93** (2016) no.5, 052002 [arXiv:1509.07152 [hep-ex]].

[18] R. Barbier *et al.*, Phys. Rept. **420** (2005) 1 [hep-ph/0406039].

[19] V. A. Mitsou, PoS **PLANCK 2015** (2015) 085 [arXiv:1510.02660 [hep-ph]] and references therein.

[20] ATLAS Collaboration, ATLAS-CONF-2016-075 (2016).

[21] ATLAS Collaboration, ATLAS-CONF-2016-057 (2016).

[22] ATLAS Collaboration, ATLAS-CONF-2016-094 (2016).

[23] ATLAS Collaboration, ATLAS-CONF-2016-084 (2016).